Effective dielectric constant of dilute suspensions of spheres

B. U. Felderhof
Institut für Theoretische Physik A, Rheinisch-Westfälische Technische Hochschule Aachen, Templergraben 55, 5100 Aachen, Federal Republic of Germany

R. B. Jones
Queen Mary College, University of London, Mile End Road, London E1 4NS, Great Britain
(Received 15 August 1988)

We study suspensions of metallic spheres randomly distributed in an insulating matrix. The effective dielectric constant of such a system is given by a Bergman representation. The positive spectral density in this representation is characteristic of the geometry and is directly related to the optical-absorption spectrum. We study the spectral density on the basis of a recently derived expression for the effective dielectric constant.

I. INTRODUCTION

Composite systems consisting of spherical metal particles embedded in an insulating matrix show interesting absorption spectra. They exhibit a strong maximum at optical frequencies which is absent in the bulk metal. For very dilute suspensions the absorption maximum can be attributed to the dipolar plasma mode of individual spheres. At higher concentrations plasma modes of different spheres couple in a way dependent on the geometrical distribution of the particles. The effects are particularly dramatic when aggregates are formed.[1-4] In this paper we concentrate on suspensions with well-separated particles. In such suspensions one expects a red shift of the spectrum with respect to the prediction of the simple Maxwell Garnett theory.[5-9] The experimental situation at present is confused.[10,11] In this article we study the spectrum from a theoretical point of view.

The effective dielectric constant of a two-phase composite may, in general, be cast in an analytic form due to Bergman.[12] In this Bergman representation $\epsilon_{\rm eff}$ is expressed in terms of a positive spectral density which is characteristic of the geometry. We assume that the spherical particles are randomly distributed with hard-sphere statistics. We study the Bergman spectral density on the basis of an expression for the effective dielectric constant for a system of spheres derived recently by Cichocki and Felderhof.[13] We approximate the exact expression by limiting our analysis to two-body electrical interactions. We expect that our results yield an accurate representation of the true spectrum up to volume fractions of about 3%.

In earlier work[7,8] we have studied the same system on the basis of a cluster expansion[14] of the effective dielectric constant. We showed that a truncation of the cluster expansion at the two-sphere level leads to a violation of the Bergman representation. We remedied the situation by introducing cutoffs in such a way that Bergman's theorem is satisfied. The new expression for $\epsilon_{\rm eff}$ does not have this difficulty and we find that on the two-sphere level the Bergman representation is automatically satisfied. Many of the results of our earlier work can be used in the present analysis.

We find a spectral density with an extremely rich structure. Already in the dipole approximation the spectrum has remarkable features. The corrections from higher-order multipoles are difficult to calculate, but lead to additional structure.

II. EFFECTIVE DIELECTRIC CONSTANT

We consider a suspension of identical spherical inclusions of radius a embedded in a uniform background medium with dielectric constant ϵ_1. The inclusions are also uniform and have dielectric constant ϵ_2. For a particular configuration the local dielectric constant is given by

$$\epsilon(\mathbf{r})=\epsilon_1[1-\Theta(\mathbf{r})]+\epsilon_2\Theta(\mathbf{r}) , \tag{2.1}$$

where $\Theta(\mathbf{r})$ is the characteristic function of the set of spheres. We assume that the disordered geometry of the system is described by a known probability distribution and that on average the suspension is uniform and isotropic.

We are interested in the effective dielectric constant $\epsilon_{\rm eff}$ of the suspension which is defined as follows. When a particular configuration is subjected to an applied electric field at frequency ω, a field $\mathbf{E}(\mathbf{r})$ with a complicated spatial dependence is set up. Both ϵ_1,ϵ_2 and the field depend on frequency, but we do not indicate this dependence explicitly. The local dielectric displacement is

$$\mathbf{D}(\mathbf{r})=\epsilon(\mathbf{r})\mathbf{E}(\mathbf{r}) . \tag{2.2}$$

We introduce the induced polarization, relative to the medium in the absence of inclusions, via the relation

$$\mathbf{D}(\mathbf{r})=\epsilon_1\mathbf{E}(\mathbf{r})+4\pi\mathbf{P}(\mathbf{r}) . \tag{2.3}$$

Averaging over the statistical ensemble of configurations we obtain

$$\langle\mathbf{D}(\mathbf{r})\rangle=\epsilon_1\langle\mathbf{E}(\mathbf{r})\rangle+4\pi\langle\mathbf{P}(\mathbf{r})\rangle . \tag{2.4}$$

In contrast to the fields in (2.3) the average fields in (2.4) are slowly varying functions of position. At sufficiently long wavelengths the average fields are related by the local constitutive equation

$$\langle \mathbf{D}(\mathbf{r})\rangle = \epsilon_{\text{eff}} \langle \mathbf{E}(\mathbf{r})\rangle \ , \tag{2.5}$$

where ϵ_{eff} is the effective dielectric constant.

In writing (2.5) we have not only assumed the suspension to be statistically isotropic, but also that we need not distinguish between longitudinal and transverse fields. The latter assumption is justified only if retardation effects may be neglected on the microscopic length scale. This requires that the sphere diameter, the mean distance between spheres, and the correlation length are all much smaller than the wavelength. We shall assume that these conditions are satisfied. As a consequence the effective dielectric constant ϵ_{eff} may be evaluated from electrostatics. The basic equations on the microscopic level may therefore be simplified to

$$\nabla \cdot \mathbf{D}(\mathbf{r}) = 4\pi \rho_0(\mathbf{r}), \quad \nabla \times \mathbf{E}(\mathbf{r}) = 0 \ , \tag{2.6}$$

where $\rho_0(\mathbf{r})$ is the external charge density. Subject to validity of the above assumptions the effective dielectric constant ϵ_{eff} may be used in the complete set of Maxwell's equations for the average fields.

It has been shown by Bergman[4] that, provided Maxwell's equations of electrostatics hold, the effective dielectric constant of the suspension has the representation

$$\epsilon_{\text{eff}} = \epsilon_1 \left[1 - \int_0^1 \frac{g(u)}{t-u} du \right] \ , \tag{2.7}$$

where the variable t is defined by

$$t = \epsilon_1/(\epsilon_1 - \epsilon_2) \ , \tag{2.8}$$

and where $g(u)$ is a positive spectral density. The spectral density is fully determined by the random geometry of the two-phase medium. Quite generally, for a system which on average is uniform the total weight of the spectral density is

$$\int_0^1 g(u) du = \phi \ , \tag{2.9}$$

where ϕ is the volume fraction of phase 2. If in addition the system on average is isotropic, then the first moment of the spectral density is given by

$$\int_0^1 u g(u) du = \tfrac{1}{3}\phi(1-\phi) \ . \tag{2.10}$$

If we approximate the spectral density by a δ function with weight and location such that the sum rules (2.9) and (2.10) are satisfied, then (2.7) leads to the Clausius-Mossotti (CM) or Maxwell Garnett formula. Explicitly,

$$g_{\text{CM}}(u) = \phi \delta(u - \tfrac{1}{3}(1-\phi)) \tag{2.11}$$

leads to

$$\epsilon_{\text{CM}} = \epsilon_1 \left[1 + \frac{3\phi}{1-\phi-3t} \right] \ . \tag{2.12}$$

In the thermodynamic limit of an infinite uniform system of spheres the spectral density may in principle be expressed in terms of the density and spatial correlation functions of the spheres. If n is the number density, then $\phi = \frac{4}{3}\pi n a^3$, and (2.11) may be regarded as a first approximation to the spectrum. A detailed statistical theory for the effective dielectric constant will lead to a more complicated spectral density. In the following we shall investigate $g(u)$ and ϵ_{eff} on the basis of a recently derived exact expression.[13]

III. SPECTRAL DENSITY

In this section we derive a general expression for the spectral density $g(u)$ occurring in the Bergman representation (2.7). It has been shown by Cichocki and Felderhof[13] on the basis of an exact resummation of multiple-scattering processes that for a disordered system of spherical particles the effective dielectric constant is given by

$$\epsilon_{\text{eff}} = \epsilon_1 + 4\pi n \alpha \left[1 - \frac{4\pi}{3\epsilon_1}(1+\lambda+\mu) n\alpha \right]^{-1} \ , \tag{3.1}$$

where α is the dipole polarizability of a single particle and λ and μ may be expressed as sums of cluster integrals. For a uniform sphere the dipole polarizability is given by

$$\alpha = \epsilon_1 \frac{\epsilon_2 - \epsilon_1}{\epsilon_2 + 2\epsilon_1} a^3 = \frac{\epsilon_1 a^3}{1-3t} \ , \tag{3.2}$$

which is singular at $t = \frac{1}{3}$. The coefficients λ and μ in (3.1) may be expressed as the sums

$$\lambda = \sum_{s=2}^{\infty} \lambda_s, \quad \mu = \sum_{s=2}^{\infty} \mu_s \ , \tag{3.3}$$

where λ_s and μ_s each are given by a cluster integral involving the solution of the electrostatic equations (2.6) for s spheres in a uniform applied electric field. Substituting (3.2) in (3.1) and comparing with (2.12) we see that the coefficients λ and μ provide corrections to the Clausius-Mossotti formula. In this paper we shall consider in particular the two-sphere contributions λ_2 and μ_2, and neglect all higher-order terms in (3.3). This must be regarded as an approximation which is valid at low density, but becomes less accurate for more concentrated systems. The approximation might be improved by including the three-sphere contributions λ_3 and μ_3, but we shall not consider these here.

Expression (3.1) may be cast in the form

$$\epsilon_{\text{eff}} = \epsilon_1 + 4\pi n \alpha'' \ , \tag{3.4}$$

with the effective polarizability

$$\alpha'' = \alpha \left[1 - \frac{4\pi}{3\epsilon_1}(1+\lambda+\mu) n\alpha \right]^{-1} \ . \tag{3.5}$$

In analogy to (3.2) this may be expressed as

$$\alpha'' = \epsilon_1 a^3/[1-\phi-3t-C(t)] \ , \tag{3.6}$$

where $C(t)$ gives the correction to the Clausius-Mossotti formula, as may be seen from (2.12). It is given by

$$C(t)=\phi(\lambda+\mu) , \tag{3.7}$$

and in the two-body approximation is approximated by

$$C_2(t)=\phi(\lambda_2+\mu_2) . \tag{3.8}$$

From (3.4) and (3.6) we find

$$\epsilon_{\text{eff}}(t)=\epsilon_1\left[1+\frac{3\phi}{1-\phi-3t-C(t)}\right] . \tag{3.9}$$

The spectral density in the Bergman representation (2.7) may be obtained from

$$g(u)=\text{Im}[\epsilon_{\text{eff}}(u+i\delta)/\pi\epsilon_1] , \tag{3.10}$$

where δ is infinitesimally positive. From (3.9) we find

$$g(u)=\frac{3\phi}{\pi}\frac{C''(u)}{[1-\phi-3u-C'(u)]^2+[C''(u)]^2} , \tag{3.11}$$

where $C'(u)$ and $C''(u)$ are defined by

$$C(u+i\delta)=C'(u)+iC''(u) . \tag{3.12}$$

We shall denote the spectral density $g(u)$ evaluated with $C(u)$ approximated by the two-sphere approximation (3.8) by $g_2(u)$.

IV. TWO-SPHERE APPROXIMATION

In this section we consider the function $C_2(t)$ in more detail. The explicit expression is

$$C_2(t)=(1-3t)^2\epsilon_{\text{eff}}(1,2)/(3\phi\epsilon_1) , \tag{4.1}$$

where the pair term $\epsilon_{\text{eff}}(1,2)$ is given by[15]

$$\epsilon_{\text{eff}}(1,2)=\frac{(4\pi)^2}{3}\int_{2a}^{\infty} dR\, R^2 n(1,2) \times[\epsilon_1 a^3 a_{10}(R) +2\epsilon_1 a^3 a_{11}(R)-3\alpha] , \tag{4.2}$$

where R is the distance between centers of the two spheres, $n(1,2)$ is the pair distribution function, and $a_{1m}(R)$ for $m=0,1$ are dimensionless pair polarizabilities. These are obtained as solutions of the coupled multipole equations

$$\sum_{l'=1}^{\infty} M_{ll'}^{m} a_{l'm}=\delta_{l1}, \quad l=1,2,\ldots \tag{4.3}$$

with matrix elements

$$M_{ll'}^{m}=\frac{\epsilon_1 a^{2l+1}}{\alpha_l}\delta_{ll'}-(-1)^m\begin{bmatrix} l+l' \\ l+m \end{bmatrix}\left[\frac{a}{R}\right]^{l+l'+1} , \tag{4.4}$$

where the multipole polarizabilities α_l are given by

$$\alpha_l=\epsilon_1\frac{l}{l-(2l+1)t}a^{2l+1} . \tag{4.5}$$

It is easily seen that the integrand in (4.2) contains a factor α^2, which cancels the prefactor in (4.1). We write the function $C_2(t)$ given by (4.1) as a sum of three terms:

$$C_2(t)=\phi[L(t)+M(t)+H(t)] , \tag{4.6}$$

where we evaluate $L(t)$ by approximating the pair distribution $n(1,2)$ in (4.2) by n^2 and by using the dipole approximation in (4.3), and $M(t)$ by again approximating $n(1,2)$ by n^2 but calculating the corrections from higher-order multipoles in (4.3). The remaining contribution $H(t)$ in (4.6) is proportional to the pair correlation function $h(R)$ defined by $n(1,2)=n^2[1+h(R)]$. The latter contribution involves an integral over near distances and may be expected to be relatively small at low densities. In the next section we consider the contribution $L(t)$ in (4.6) in more detail.

V. DIPOLE APPROXIMATION AT LOW DENSITY

In this section we approximate the function $C(t)$ by $\phi L(t)$. This implies the use of the dipole approximation in (4.2). Moreover, we assume low density and approximate the pair distribution $n(1,2)$ in (4.2) by n^2 for $R>2a$. The dipole approximation to (4.2) is obtained by truncating Eqs. (4.3) at $l=1$, $l'=1$, which yields

$$a_{10}^{D}=(1-3t-2z^3)^{-1} , \quad a_{11}^{D}=(1-3t+z^3)^{-1} , \tag{5.1}$$

where $z=a/R$. The resulting integral leads to

$$L(t)=\tfrac{2}{3}\ln\left[\frac{3-8t}{2-8t}\right] . \tag{5.2}$$

It is of interest to write this in the form of a spectral representation

$$L(t)=-\tfrac{2}{3}\int_{1/4}^{3/8}\frac{du}{t-u} , \tag{5.3}$$

which shows that the corresponding spectral density is constant on the interval $\frac{1}{4}\le u\le\frac{3}{8}$. For $t=u+i\delta$ with u real and δ infinitesimally positive, the real and imaginary parts of $L(t)$ are

$$L'(u)=\tfrac{2}{3}\ln\left|\frac{3-8u}{2-8u}\right| , \quad L''(u)=\tfrac{2}{3}\pi\Theta(u;\tfrac{1}{4},\tfrac{3}{8}) , \tag{5.4}$$

where $\Theta(u;\frac{1}{4},\frac{3}{8})$ equals unity on the interval $\frac{1}{4}\le u\le\frac{3}{8}$ and vanishes elsewhere.

We denote the spectral density obtained by approximating the function $C(t)$ by $\phi L(t)$ as $g_{2D}^{(0)}(u)$, where the subscript D denotes dipole approximation and the superscript denotes low density. It is convenient to introduce the functions

$$X_D(u)=1-\phi-3u-\phi L'(u), \quad Y_D(u)=\phi L''(u) . \tag{5.5}$$

It is easily seen graphically that the function $X_D(u)$ has a zero $u_{1D}<\frac{1}{4}$ and a zero $u_{2D}>\frac{3}{8}$. These correspond to zeros on the real axis of the denominator in (3.9). Hence, in the present approximation the spectral density is given by

$$g_{2D}^{(0)}(u)=\phi A_{1D}\delta(u-u_{1d})+\frac{3\phi}{\pi}\frac{Y_D(u)}{X_D^2(u)+Y_D^2(u)}$$
$$+\phi A_{2D}\delta(u-u_{2D}) \tag{5.6}$$

with amplitudes A_{1D} and A_{2D} given by

$$A_{jD}=-3/(dX_D/du)_{u_{jD}},\quad j=1,2\ . \tag{5.7}$$

From (5.5) we find explicitly

$$dX_D/du=-3-\tfrac{16}{3}\phi[(2-8u)(3-8u)]^{-1}\ . \tag{5.8}$$

In Fig. 1 we plot u_{1D} and u_{2D} as a function of the volume fraction and in Fig. 2 we plot the amplitudes A_{1D} and A_{2D} in the same range, $0<\phi<0.2$. Note that according to the normalization (2.9) the amplitudes A_{1D} and A_{2D} give the relative contributions of the isolated modes at u_{1D} and u_{2D} to the spectral density. It is remarkable that at the higher volume fractions these modes carry a substantial portion of the total weight.

It follows from (5.4) and (5.5) that the continuous contribution to $g_{2D}^{(0)}(u)$ given by the second term in (5.6) is maximum at a zero of $X_D(u)$ and then takes the value $9/2\pi^2\approx0.456$ independent of the volume fraction. It is easily shown that for $0<\phi\lesssim0.091$ the function $X_D(u)$ has three zeros in the interval $[\frac{1}{4},\frac{3}{8}]$. Thus for small volume fractions the function $g_{2D}^{(0)}(u)$ shows three sharp peaks in the interval $[\frac{1}{4},\frac{3}{8}]$. For $\phi\approx0.091$ two zeros of $X_D(u)$ coalesce so that for $0.091\lesssim\phi<9/64$ the graph of $g_{2D}^{(0)}(u)$ shows two broad maxima, while for $\phi>\frac{9}{64}$ only one maximum remains near $u=\frac{3}{8}$. In Fig. 3 we plot $g_{2D}^{(0)}(u)$ on the interval $[\frac{1}{4},\frac{3}{8}]$ for five volume fractions between 0.02 and 0.08. In Fig. 4 we plot the same for volume fractions 0.11, $\frac{9}{64}$, and 0.2. Note that the total weight carried by the continuous part of the spectrum is bounded by $9/16\pi^2\approx0.057$, since the function takes the maximum value $9/2\pi^2$. The remainder of the total weight ϕ must be carried by the two delta functions in (5.6).

In the present approximation we find that the spectral density has striking features, namely two isolated modes

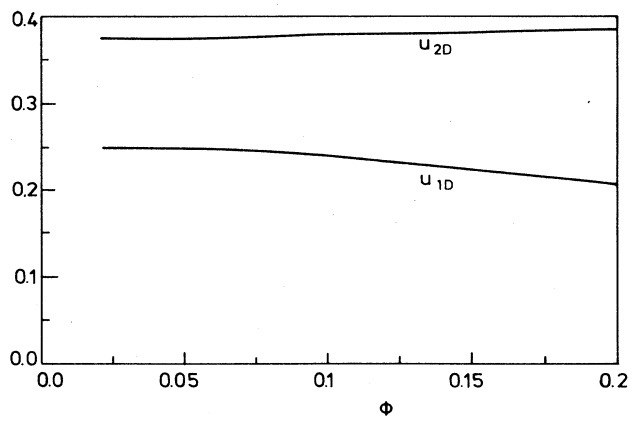

FIG. 1. Plot of the zero $U_{1D}<\frac{1}{4}$ of $X_D(u)$ and of the zero $u_{2D}>\frac{3}{8}$.

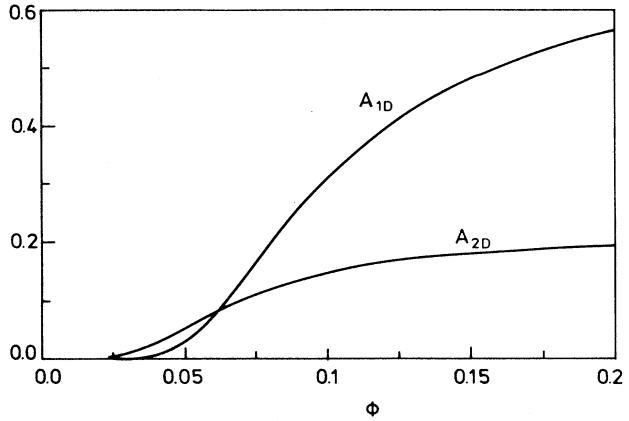

FIG. 2. Plot of the amplitudes A_{1D} and A_{2D}.

at $u_{1D}<\frac{1}{4}$ and $u_{2D}>\frac{3}{8}$ and a continuous spectrum in the interval $\frac{1}{4}\le u\le\frac{3}{8}$. In the next two sections we investigate how the spectrum is modified by multipolar interactions.

VI. MULTIPOLE CONTRIBUTIONS AT LOW DENSITY

In this section we study the function $M(t)$ defined in (4.6) in order to understand how its contribution affects the spectral density $g(u)$. The multipole contribution to the integral in (4.2) is found from the coefficients b_{1m} defined by

$$b_{1m}=a_{1m}-a_{1m}^{D}\ . \tag{6.1}$$

This yields

$$M(t)=(1-3t)^2\int_0^{1/2}\frac{dz}{z^4}[b_{10}(t,z)+2b_{11}(t,z)]\ . \tag{6.2}$$

As shown previously,[15] the coefficients b_{1m} are given by

$$b_{1m}=-(M_{11}^{m})^{-1}\frac{\det(\tilde{M}^{m})}{\det(M^{m})}\ , \tag{6.3}$$

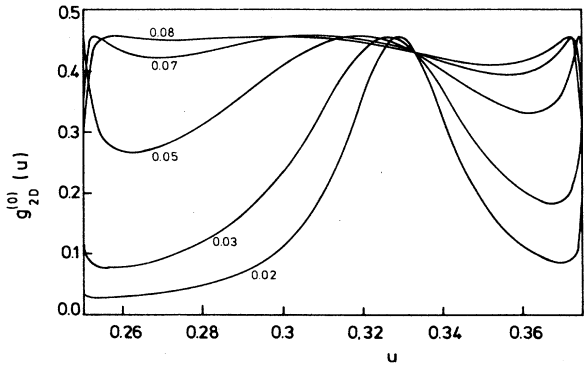

FIG. 3. Plot of the spectral density $g_{2D}^{(0)}(u)$ on the interval $[\frac{1}{4},\frac{3}{8}]$ for volume fractions 0.02, 0.03, 0.05, 0.07, and 0.08.

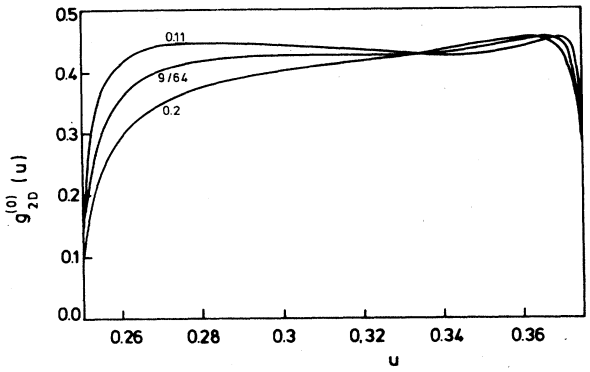

FIG. 4. Same plot as in Fig. 3 for volume fractions 0.11, $\frac{9}{64}$, and 0.2.

where the matrix $\tilde{M}^{m}$ has elements

$$\tilde{M}^{m}_{ll'}=(1-\delta_{l1}\delta_{l'1})M^{m}_{ll'} \ . \tag{6.4}$$

At distances R close to the sphere diameter $2a$ ($z\approx\frac{1}{2}$) a large number of multipoles must be taken into account. It turns out that by use of the formula (6.3) the integral in (6.2) may be evaluated with good numerical accuracy, unless the point t in the complex t plane is very close to that part of the real interval [0,1], where the spectral density is located. Unfortunately this means that a direct study of the contribution of $M(t)$ to the spectral density $g(u)$ based on (6.2) and (6.3) is not possible.

An alternative approach can be based on the fact, shown in Ref. 8, that $M(t)$ itself has a spectral representation

$$M(t)=-\tfrac{1}{3}(1-3t)^2\int_0^1\frac{\hat{m}(u)}{t-u}du \ , \tag{6.5}$$

with a real function $\hat{m}(u)$. We have seen in (5.4) that the dipole contribution $L(t)$ has a spectral density confined to the narrow interval $[\frac{1}{4},\frac{3}{8}]$. We expect that the higher multipoles will have the effect of spreading out the spectral density so that $\hat{m}(u)$ fills the interval [0,1]. To test this we have numerically calculated $\hat{m}(u)$ in quadrupole approximation.

The quadrupole approximation is defined by truncating Eqs. (4.3) at $l=2$, $l'=2$, which yields

$$\begin{aligned} a^{Q}_{10}&=[1-3t-2z^3-9z^8(1-\tfrac{5}{2}t-6z^5)^{-1}]^{-1} \ , \\ a^{Q}_{11}&=[1-3t+z^3-3z^8(1-\tfrac{5}{2}t+4z^5)^{-1}]^{-1} \ . \end{aligned} \tag{6.6}$$

We define coefficients $b^{Q}_{lm}=a^{Q}_{lm}-a^{D}_{lm}$ and it then follows from (5.1) and (6.6) that the b^{Q}_{lm} can be written as

$$b^{Q}_{lm}(t,z)=\frac{-2z^8}{5(2m+1)[t-h_{1m}(z)][t-h_{2m}(z)][t-h_{3m}(z)]} \ , \tag{6.7}$$

where

$$\begin{aligned} h_{10}(z)&=\tfrac{1}{3}(1-2z^3) \ , \\ h_{11}(z)&=\tfrac{1}{3}(1+z^3) \ , \\ h_{2m}(z)&=d_{1m}+[d^2_{1m}(z)-d_{2m}(z)]^{1/2} \ , \\ h_{3m}(z)&=d_{1m}-[d^2_{1m}(z)-d_{2m}(z)]^{1/2} \ , \end{aligned} \tag{6.8}$$

with

$$\begin{aligned} d_{10}(z)&=\frac{11}{30}-\frac{z^3}{3}-\tfrac{6}{5}z^5 \ , \\ d_{20}(z)&=\tfrac{2}{15}(1-2z^3-6z^5+3z^8) \ , \\ d_{11}(z)&=\frac{11}{30}+\frac{z^3}{6}+\tfrac{4}{5}z^5 \ , \\ d_{21}(z)&=\tfrac{2}{15}(1+z^3+4z^5+z^8) \ . \end{aligned} \tag{6.9}$$

We can resolve $b^{Q}_{lm}(t,z)$ into partial fractions by the formula

$$\begin{aligned} [(t-h_{1m})(t-h_{2m})(t-h_{3m})]^{-1}&=(h_{1m}-h_{2m})^{-1}(h_{1m}-h_{3m})^{-1}(t-h_{1m})^{-1} \\ &+(h_{2m}-h_{3m})^{-1}(h_{2m}-h_{1m})^{-1}(t-h_{2m})^{-1} \\ &+(h_{3m}-h_{1m})^{-1}(h_{3m}-h_{2m})^{-1}(t-h_{3m})^{-1} \ . \end{aligned} \tag{6.10}$$

From (6.5) and (6.2) we have

$$\int_0^1\frac{\hat{m}(u)}{t-u}du=-3\int_0^{1/2}\frac{dz}{z^4}[b_{10}(t,z)+2b_{11}(t,z)] \ . \tag{6.11}$$

Upon inserting the partial-fraction resolution of $b^{Q}_{lm}(t,z)$ into (6.11), we obtain $\hat{m}^{Q}(u)$, the quadrupole contribution to the multipole spectral density, expressed parametrically in terms of z. For example, one of the six contributions to (6.11) has the form

$$\tfrac{4}{5}\int_0^{1/2}\frac{z^4}{[h_{21}(z)-h_{11}(z)][h_{21}(z)-h_{31}(z)]}\frac{dz}{t-h_{21}(z)} \ ,$$

from which we deduce that on the interval $h_{21}(0)<u<h_{21}(\frac{1}{2})$ [$h_{21}(0)=\frac{2}{5}$, $h_{21}(\frac{1}{2})=(33+\sqrt{19})/80=0.467$],

$$\hat{m}^{Q}(u)=\frac{4z^4}{5h'_{21}(z)[h_{21}(z)-h_{11}(z)][h_{21}(z)-h_{31}(z)]} \ , \tag{6.12}$$

where $h'_{21}(z)=dh_{21}(z)/dz$ and $z=h^{-1}_{21}(u)$.

There are six contributions like (6.12), some of which overlap on the u axis. Moreover, there is a weak singularity in $\hat{m}^{Q}(u)$ at $u=\frac{1}{3}$ which we have resolved by using

computer algebra to invert the various functions concerned,

$$\hat{m}^{Q}(u)=24(3u-1)^{-1/3}+120(3u-1)^{2/3}-360(3u-1)^{4/3}+\cdots,\quad u\to\tfrac{1}{3}^{+}$$
$$\hat{m}^{Q}(u)=-9\left[\frac{2}{1-3u}\right]^{1/3}+90\left[\frac{1-3u}{2}\right]^{2/3}-\frac{405}{2}\left[\frac{1-3u}{2}\right]^{4/3}+\cdots,\quad u\to\tfrac{1}{3}^{-}. \tag{6.13}$$

We display $\hat{m}^{Q}(u)$ graphically in Fig. 5. The quadrupole spectral density $\hat{m}^{Q}(u)$ extends from $u=(23-\sqrt{39})/80=0.209$ to $u=(33+\sqrt{19})/80=0.467$, a significantly larger interval than [0.250, 0.375], on which the dipole spectral density is concentrated. Note also that in addition to the weak singularity mentioned above, there are step discontinuities in $\hat{m}^{Q}(u)$ at several places.

The quadrupole contributions do not exhaust the effects of higher multipoles. Although we are unable to handle multipoles higher than $l=2$ in the same detail as the quadrupole, we were able, by computer algebraic manipulation, to determine the width of the multipole spectral density when Eqs. (4.3) are truncated at $l=l'=3$ and at $l=l'=4$. Upon including octupoles the multipole spectral density is nonvanishing on the interval [0.179, 0.527] and for $l=4$ multipoles this broadens further to [0.155, 0.574].

Although we cannot include multipoles for $l>2$ in an explicit way, it is possible to incorporate them approximately, for all $l>2$, by a method of moments. In (6.5) we can expand the integral as a series of inverse powers of t,

$$\int_0^1 \frac{\hat{m}(u)}{t-u}du=\sum_{j=1}^{\infty}\hat{m}_j t^{-j}, \tag{6.14}$$

where the coefficients $\hat{m}_j$ are given by the moments of the spectral density $\hat{m}(u)$,

$$\hat{m}_j=\int_0^1 u^{j-1}\hat{m}(u)du. \tag{6.15}$$

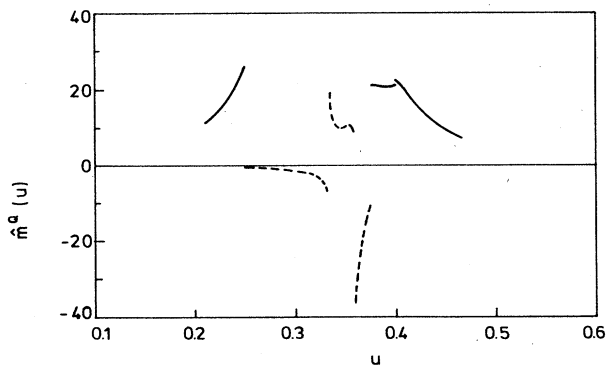

FIG. 5. Plot of the spectral density $\hat{m}^{Q}(u)$. On the dashed curve the actual values have been reduced by a factor 10.

The first two moments $\hat{m}_1$ and $\hat{m}_2$ vanish identically. The moment $\hat{m}_3$ is given exactly by[8]

$$\hat{m}_3=\tfrac{7}{108}-\tfrac{1}{24}\ln 3\approx 0.019\,039, \tag{6.16}$$

while the moment $\hat{m}_4$ was shown to be

$$\hat{m}_4\approx 0.019\,242. \tag{6.17}$$

We have extended the moment calculation by a method presented in the Appendix to obtain two additional moments:

$$\hat{m}_5\approx 0.013\,551,\quad \hat{m}_6\approx 0.008\,292. \tag{6.18}$$

These moments contain the contributions of all multipoles for $l\geq 2$. We split off the quadrupole contributions explicitly by writing

$$\hat{m}(u)=\hat{m}^{Q}(u)+\hat{m}^{R}(u), \tag{6.19}$$

where $\hat{m}^{R}(u)$ contains the contributions for $l>2$. By computer algebra we expanded the b^0_{1m} in a series of inverse powers of t and then used (6.11) and (6.14) to evaluate the quadrupole contribution to the moments $\hat{m}_i$. This gave the following result for the contribution of $\hat{m}^{R}(u)$ to the moments $\hat{m}_3,\ldots,\hat{m}_6$,

$$\hat{m}^{R}_3=0.006\,540,\quad \hat{m}^{R}_4=0.006\,585,\quad \hat{m}^{R}_5=0.004\,848,\quad \hat{m}^{R}_6=0.003\,219. \tag{6.20}$$

A finite number of moments do not uniquely specify $\hat{m}^{R}(u)$, but they can be used to determine a coarse-grained representation of it. We choose to represent $\hat{m}^{R}(u)$ by an expansion in Jacobi polynomials,[16]

$$\hat{m}^{R}(u)=w(p,q,u)\sum_{j=2}^{5}c_j G_j(p,q,u), \tag{6.21}$$

where $w(p,q,u)$ is the weight function,

$$w(p,q,u)=u^{q-1}(1-u)^{p-q}. \tag{6.22}$$

The Jacobi polynomials $G_n(p,q,u)$ constitute the set of orthogonal polynomials with respect to the weight function $w(p,q,u)$ on the interval $0\leq u\leq 1$. Due to absence in (6.21) of the terms G_0 and G_1 the sum rules $\hat{m}^{R}_1=0$ and $\hat{m}^{R}_2=0$ are satisfied automatically. The coefficients $c_2,\ldots,c_5$ are fixed by requiring that $\hat{m}^{R}(u)$ have the correct moments $\hat{m}^{R}_3,\ldots,\hat{m}^{R}_6$. We center the weight function at $u=\frac{1}{3}$ by setting $p=3q-2$. Finally, to determine q we evaluate the integral (6.5) for a range of t values off the u axis using numerical values of $\hat{m}^{Q}(u)$ and the representation of $\hat{m}^{R}(u)$ in (6.21). These values of the integral are compared with values computed using (6.2) and (6.3) and given in an earlier paper.[8] The best fit corresponds to $q=13.5$. We show the graph of $\hat{m}^{R}(u)$ in Fig. 6. We observe that $\hat{m}^{R}(u)$ is negligibly small outside the interval [0.1, 0.65]. Our representation of the multipole spectral density, $\hat{m}(u)=\hat{m}^{Q}(u)+\hat{m}^{R}(u)$, and hence of $M(t)$ itself, is now uniquely determined. We have found that the spectral density $\hat{m}(u)$ is spread over a much wider range than the dipole spectral function $L''(u)$, and the quadrupole contributions give much more structure to $\hat{m}(u)$ than is evident in $L''(u)$.

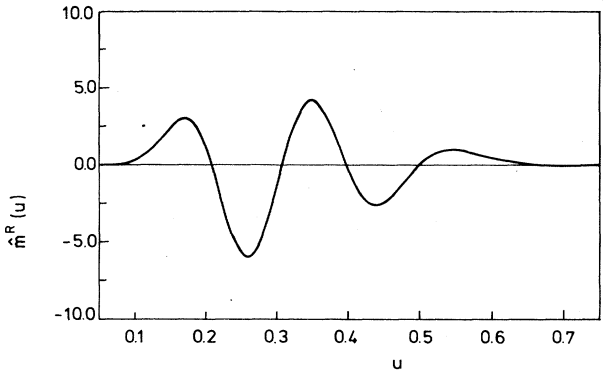

FIG. 6. Plot of the spectral density $\hat{m}^R(u)$.

VII. SPECTRAL DENSITY INCLUDING MULTIPOLE CONTRIBUTIONS

In this section we include the multipolar function $M(t)$ given by (6.5) and (6.19) in the calculation of the effective dielectric constant and the spectral density. We approximate $C_2(t)$ in (4.6) by $\phi[L(t)+M(t)]$ and use (3.9) to evaluate $\epsilon_{\text{eff}}(t)$. For values $u+i\delta$ with u real and δ infinitesimally positive ϵ_{eff} is given by

$$\epsilon_{\text{eff}}(u+i\delta)\approx\epsilon_1\left[1+\frac{3\phi}{X(u)-iY(u)}\right] \tag{7.1}$$

with the function $X(u)$ defined by

$$X(u)=1-\phi-3u-\phi[L'(u)+M'(u)] \tag{7.2}$$

and the function $Y(u)$ defined by

$$Y(u)=\phi[L''(u)+M''(u)]\ . \tag{7.3}$$

From (6.5) we find, for the multipolar contributions,

$$\begin{aligned} M'(u)&=-\tfrac{1}{3}(1-3u)^2\mathrm{P}\int_0^1\frac{\hat{m}(v)}{u-v}dv\ , \\ M''(u)&=\tfrac{1}{3}\pi(1-3u)^2\hat{m}(u)\ , \end{aligned} \tag{7.4}$$

where P indicates the principal-value integral.

Using (3.10) we find that the spectral density $g(u)$ at low concentration and in the two-sphere approximation is given by

$$g_2^{(0)}(u)=\frac{3\phi}{\pi}\frac{Y(u)}{X^2(u)+Y^2(u)}\ . \tag{7.5}$$

It is clear from (7.3) and (7.4) that the function $Y(u)$ now no longer vanishes outside the interval $[\frac{1}{4},\frac{3}{8}]$. Due to the multipolar interactions we obtain a spectral density which in principle is spread through the interval [0,1]. Our representation of $\hat{m}(u)=\hat{m}^Q(u)+\hat{m}^R(u)$ as an explicit quadrupole contribution plus a smooth representation of all higher multipoles should give a good coarse-grained representation of the two-body interactions, but also leads to specific features of $g_2^{(0)}(u)$ related to the separation of quadrupole contributions into an isolated term $\hat{m}^Q(u)$.

In the preceding section we found that $\hat{m}^Q(u)$ was characterized by a weak singularity at $u=\frac{1}{3}$ and by several jump discontinuities. Because of the factor $(1-3u)^2$ in (7.4) the singularity has no observable effect on $M(u+i\delta)$. More importantly, we observe that at all points of discontinuity where $\hat{m}^Q(u)$ is not vanishing, the principal-value integral in $M'(u)$ diverges logarithmically. This phenomenon is already manifest in the dipole term where the divergence in $L'(u)$ at $u=\frac{1}{4},\frac{3}{8}$ reflects the discontinuity in $L''(u)$ at these points. At such points $X(u)$ also diverges forcing $g_2^{(0)}(u)$ to vanish at these points. One can easily see by a graphic argument that near such a divergence there must also be a zero of $X(u)$ analogous to the vanishing denominator in (3.9) which produced the isolated modes in $g_{2D}^{(0)}(u)$. In the present instance there can be no such sharp modes because of the fact that $\hat{m}^R(u)$ is, apart from isolated points, nonzero throughout [0,1]. Nevertheless, depending on the value of $Y(u)$ near such zeros of $X(u)$, there may be sharp peaks in $g_2^{(0)}(u)$ associated with such zeros. A graph of $g_2^{(0)}(u)$ for a volume fraction $\phi=0.03$ is shown in Fig. 7. The zeros of $g_2^0(u)$ associated with divergencies of $X(u)$ are indicated, including those at $\frac{1}{4}$ and $\frac{3}{8}$ due to the dipole contribution $L'(u)$. The spectral density is still dominated by a single peak as in the dipole approximation and this peak corresponds to a zero of $X(u)$ at about 0.327. There is a secondary peak in $g_2^{(0)}(u)$ at about $u=0.36$ which is due to quadrupole interaction and which reflects the structure in $\hat{m}^Q(u)$ near 0.358 where it has a strong discontinuity as shown in Fig. 5. At higher volume fractions $g_2^{(0)}(u)$ shows even more structure with the main peak shifting to lower u values and with additional secondary peaks appearing at higher values of u. However, in these more dense systems it is likely that three-body terms begin to contribute significantly so that $g_2^{(0)}(u)$ gives only a rough idea of the actual spectral density.

The detailed structure of $g_2^{(0)}(u)$ as described above is approximate owing to the smoothed representation of the higher multipoles by $\hat{m}^R(u)$. Nonetheless, we see from the form of $L''(u)$ and $\hat{m}^Q(u)$ that there is a competition between the contributions of different multipoles which alters as u varies. The zeros of $g_2^{(0)}(u)$ which are forced

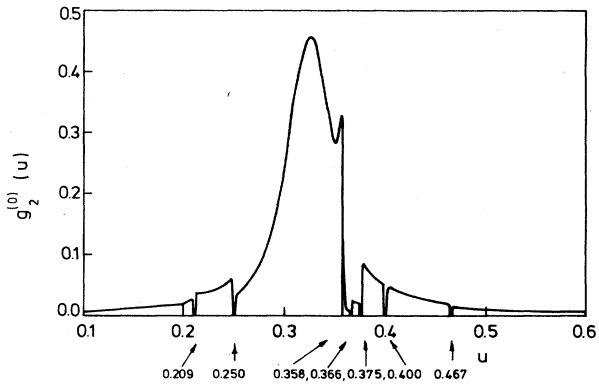

FIG. 7. Plot of the spectral density $g_2^{(0)}(u)$ at volume fraction $\phi=0.03$. The zeros of the spectral density are indicated.

by the divergence of $X(u)$ arising from specific contributions are probably a general feature of the exact $g(u)$; however, it is unlikely that such detailed features can be resolved by experimental measurements at t values off the real axis.

VIII. RELATION TO EXPERIMENT

Our investigation of the spectral function $g(u)$ leads to definite predictions for the effective dielectric constant of suspensions of spheres. The systems most favorable for experimental investigation are metallic spheres embedded in a passive matrix such as glass or gelatin.[10,11] For such systems the complex variable t defined in (2.8) runs along a path in the complex t plane starting at zero frequency and passing close by the interval [0,1]. For example, the Drude model for the dielectric constant $\epsilon_2(\omega)$ of metallic spheres yields

$$\epsilon_2(\omega)=\epsilon_{2\infty}'+i\epsilon_{2\infty}''-\frac{\omega_p^2}{\omega(\omega+i\gamma)} \tag{8.1}$$

with $\epsilon_{2\infty}'=4.5$, $\epsilon_{2\infty}''=0.16$, $\omega_p=1.46\times10^{16}$ s^{-1}, $\gamma=1.68\times10^{14}$ s^{-1} for silver spheres of radius 100 Å. The imaginary part $\epsilon_{2\infty}''$ represents the effect of interband contributions which would arise in a quantum-mechanical microscopic calculation of $\epsilon_2(\omega)$. With $\epsilon_1=2.25$ for glass this leads to $t'=\frac{1}{3}$ and $t''=0.023$ at the single-sphere resonance frequency $\omega_s=4.87\times10^{15}$ s^{-1}. In Fig. 1 of Ref. 3 we have presented a plot of the path in the complex t plane. For such a system one can expect to see the details of the spectral density $g(u)$. In Fig. 8 we plot the real and imaginary parts of $\epsilon_{\rm eff}(\omega)/\epsilon_1$ as a function of frequency for a system of silver spheres in glass at volume fraction $\phi=0.03$. We have used the spectral density as calculated in (7.5) and the Drude model (8.1) with parameters as given above. In Fig. 9 we present the corresponding Cole-Cole plot. There are marked deviations from the Clausius-Mossotti circle, which is drawn in the same figure for comparison.

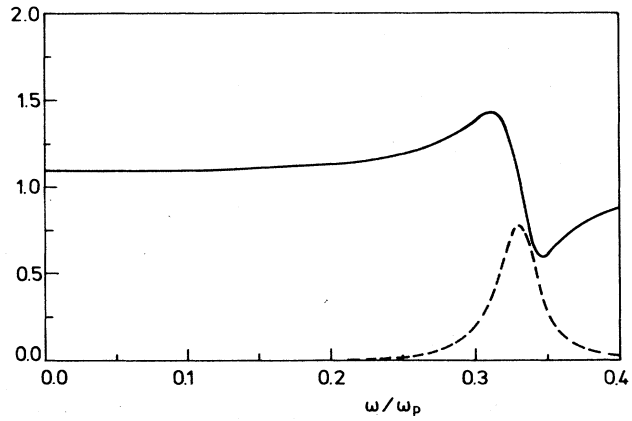

FIG. 8. Plot of the real and imaginary parts of $\epsilon_{\rm eff}(\omega)/\epsilon_1$ vs ω/ω_p for silver spheres in glass at volume fraction $\phi=0.03$.

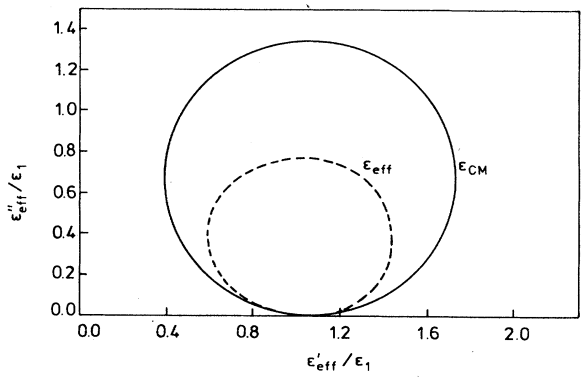

FIG. 9. Cole-Cole plot of $\mathrm{Im}\epsilon_{\rm eff}(\omega)/\epsilon_1$ vs $\mathrm{Re}\epsilon_{\rm eff}(\omega)/\epsilon_1$ for silver spheres in glass at volume fraction $\phi=0.03$ (inner curve). For comparison we also show the Clausius-Mossotti circle.

IX. DISCUSSION

We have presented a detailed calculation of the spectral density $g(u)$, defined in (2.7), for a system of spheres embedded in a matrix. We have made a two-particle approximation and therefore our results are limited to relatively low volume fraction. We have neglected the effect of correlations in the sphere positions, apart from the nonoverlap condition. This effect is represented by the function $H(t)$ in (4.6) and could be calculated, but is expected to be small at the volume fractions under consideration. We have found a spectral density with a remarkably rich structure. We expect that for volume fractions up to 0.03 our results are an accurate representation of the true spectrum.

ACKNOWLEDGMENTS

We thank the Deutsche Forschungsgemeinschaft for financial support. One of us (R.B.J.) wishes to thank the University of London Central Research Fund for a grant providing the computer software used in the symbolic calculations reported.

APPENDIX

The moments $\hat{m}_j$ defined in (6.14) are obtained from (6.11) written in the form

$$\int_0^1\frac{\hat{m}(u)}{t-u}du=-3\int_0^{1/2}\frac{dz}{z^4}\left[a_{10}(t,z)+2a_{11}(t,z)-\frac{3}{1-3t}\right]+3\int_0^{1/2}\frac{dz}{z^4}\left[a_{10}^D(t,z)+2a_{11}^D(t,z)-\frac{3}{1-3t}\right]. \tag{A1}$$

We have shown in a previous paper[7] how the coupled equations (4.3) may be solved in a series of inverse powers of t,

$$a_{lm}(t,z)=\sum_{n=1}^{\infty}c_{lmn}(z)t^{-n}, \tag{A2}$$

and the dipole coefficients a_{lm}^D have a similar representation with $c_{10n}^D = -3^{-n}(1-2z^3)^{n-1}$, $c_{11n}^D = -3^{-n}(1+z^3)^{n-1}$. Upon inserting the series expansion (A2) in (A1) and using (6.14), we obtain

$$\hat{m}_j = \Gamma_j - \Gamma_j^D , \tag{A3}$$

where

$$\Gamma_j = -3\int_0^{1/2} \frac{dz}{z^4}[c_{10j}(z)+2c_{11j}(z)+3^{1-j}] \tag{A4}$$

and similarly for Γ_j^D with c_{lmn} replaced by c_{lmn}^D.

In our earlier paper[7] we showed that $c_{lmn}(z)$ can be found in closed analytic form for $n=3,4$, giving the values of $\hat{m}_3, \hat{m}_4$. For $n>4$ no closed form can be found, but instead we represent $c_{lmn}(z)$ by a power series,

$$c_{lmn}(z) = \sum_{p=0}^{\infty} d_{lmpn} z^p . \tag{A5}$$

Upon inserting (A2) and (A5) in the coupled equations (4.3) and equating coefficients of corresponding powers of t and z, we derive a set of recurrence relations for the coefficients d_{lmpn}, when $p>0$,

$$\begin{aligned} d_{l,0,p,n+1} &= \frac{l}{2l+1} d_{l,0,p,n} - \frac{l(l+1)}{2l+1} d_{1,0,p-2-l,n} \\ &\quad - \frac{l}{2l+1} \sum_{q=0}^{p-3-l} \frac{(p-1-q)!}{l!(p-1-q-l)!} \\ &\quad \times d_{p-1-l-q,0,n} , \\ d_{l,1,p,n+1} &= \frac{l}{2l+1} d_{l,1,p,n} + \frac{l}{2l+1} d_{1,1,p-2-l,n} \\ &\quad + \frac{l}{2l+1} \sum_{q=0}^{p-3-l} \frac{(p-1-q)!}{(l+1)!(p-2-q-l)!} \\ &\quad \times d_{p-1-l-q,1,q,n} . \end{aligned} \tag{A6}$$

The input information to begin the recursive calculation of the d_{lmpn} is

$$d_{lmp1} = -\tfrac{1}{3}\delta_{l1}\delta_{p0} . \tag{A7}$$

We solved these recursion relations out to $p=50$ and then found the Γ_j for $j=5,6$ by integrating the resulting series for the $c_{lmn}(z)$ truncated at order z^{50}. This procedure gave the moments $\hat{m}_5, \hat{m}_6$ quoted in (6.18). For higher j values the method would in principle still work, but the series representation of $c_{lmn}(z)$ converges more and more slowly so that there is a progressive loss of accuracy.

[1] F. Claro and R. Fuchs, Phys. Rev. B **33**, 7956 (1986).
[2] R. Fuchs, Phys. Rev. B **35**, 7700 (1987).
[3] M. Quinten and U. Kreibig, Surf. Sci. **172**, 557 (1986).
[4] M. Ausloos, J. Phys. C **18**, L1163 (1985).
[5] B. N. J. Persson and A. Liebsch, Solid State Commun. **44**, 1637 (1982).
[6] V. A. Davis and L. Schwartz, Phys. Rev. B **33**, 6627 (1986).
[7] B. U. Felderhof and R. B. Jones, Z. Phys. B **62**, 43 (1986).
[8] B. U. Felderhof and R. B. Jones, Z. Phys. B **62**, 215 (1986).
[9] R. G. Barrera, G. Monsivais, and W. L. Mochan, Phys. Rev. B **38**, 5371 (1988).
[10] U. Kreibig, A. Althoff, and H. Pressmann, Surf. Sci. **106**, 308 (1981).
[11] W. J. Kaiser, E. M. Logothetis, and L. E. Wenger, J. Phys. C **18**, L837 (1985).
[12] D. J. Bergman, Phys. Rep. **43**, 377 (1978); Phys. Rev. B **23**, 3058 (1981).
[13] B. Cichocki and B. U. Felderhof, J. Stat. Phys. **53**, 499 (1988).
[14] B. U. Felderhof, G. W. Ford, and E. G. D. Cohen, J. Stat. Phys. **28**, 135 (1982).
[15] B. U. Felderhof, G. W. Ford, and E. G. D. Cohen, J. Stat. Phys. **28**, 649 (1982).
[16] *Handbook of Mathematical Functions,* edited by M. Abramowitz and I. A. Stegun (National Bureau of Standards, Washington, D.C., 1966), pp. 774 and 930.